A new method of refining near-earth object characteristics and behaviours using differential correction

Richard Samuel[(1)(2)]

[(1)] PhD candidate, Space Environment Research Centre, AITC2 Mount Stromlo Observatory, Cotter Road, Weston Creek, ACT 2611, AUSTRALIA
[(2)] PhD candidate, Australian National University, Research School of Astronomy & Astrophysics, Mount Stromlo Observatory, Cotter Road, Weston Creek, ACT 2611 AUSTRALIA, richard.samuel@anu.edu.au

ABSTRACT

A new method of refining the physical and behavioural characteristics of near-earth orbiting objects is being developed. The method performs orbit propagation using special perturbations and refines orbital states and characteristic parameters through differential correction until a set of constituent equations are satisfied. The method uses geophysical, atmospheric and third-body models of greater fidelity and more object characteristic parameters than are typically used in conventional forward propagation. The method is similar to cell-based engineering analyses – such as computational fluid dynamics – in that it uses constituent equations such as continuity, energy and momentum, and is solved by iterative linear algebraic techniques. To add determinacy to the system of equations for development purposes, the method is tested using three of the four accidental conjunction scenarios that have occurred to date. This paper describes the solution strategy, implementation issues and barriers to convergence.

1 INTRODUCTION

Maintaining near-earth object custody is an essential requirement for orbital collision avoidance. In this context, maintaining custody means that forward propagation will satisfactorily predict the position of objects for periods in between direct observation opportunities. However, a poor understanding of an objects' physical characteristics, such as mass, size, drag and solar radiation properties too often results in a loss of object custody. Frequently, there are more than one thousand near-earth orbiting objects for which custody has been lost for longer than thirty days, as tabled in [1]. This method aims to refine object characteristic parameters in order to increase the quality of forward propagation.

2 CONCEPTUAL BASIS

The conceptual basis of this method is similar to other cell-based engineering analyses that employ continuum mechanics. Constituent quantities are evaluated macroscopically around or through the cells and equated to adjoining cells, forming a system of equations to be solved simultaneously. For example, in computational fluid dynamics, the constituent quantities are mass continuity, fluid momentum and fluid energy. Since this method is celestially-based, the analogous constituent quantities are orbital state continuity, angular momentum and mechanical energy.

In contrast to other analyses, cells in this method do not have fixed or deforming spatial coverage; they are propagation intervals between orbital states that obey Newton's second law of motion. Hence, it should be possible to solve for the characteristic properties of near-earth orbiting objects – including mass and a supposed spherical radius – by applying universal laws of conservation to the state continuity, angular momentum and mechanical energy across a series of orbital states.

To provide determinacy to the system of equations for development and evaluation purposes, the method is being tested for three of the four historical accidental conjunctions, as documented in [2] and shown in Table 1. Orbital state information for the objects involved in the fourth case – COSMOS 926 DEB (SCC 13475) and COSMOS 1934 (SCC 18985) on 23 December 1991 – was insufficient for this purpose.

Table 1. Collision cases for evaluation

Case	Primary object	SCC	Object name	Launch date	Collision date
1	1	22675	COSMOS 2251	16 JUN 1993	10 FEB 2009
	2	24946	IRIDIUM 33	14 SEP 1997	
2	3	07219	THOR BURNER 2A R/B	16 MAR 1974	17 JAN 2005
	4	26207	CZ-4 DEB	14 OCT 1999	
3	5	18208	ARIANE 1 DEB	22 FEB 1986	24 JUL 1996
	6	23606	CERISE	7 JUL 1995	

2.1 Model suitability

Attention has been given to the use of appropriate geophysical and atmospheric models to prevent closed-loop optimisation from attempting to resolve constituent discrepancies by adjusting unrelated characteristic parameters. Best-available geophysical, atmospheric and earth orientation models – such as EGM2008, NRLMSIS-00 and IAU 2000/2006 – are employed to minimise this likelihood. The method also features a generalised discrepancy force model to represent residual forces or geophysical and atmospheric variations arising from either natural or non-natural phenomena, including manoeuvres when applicable.

2.2 Kinematic sphere of influence

The choice of an appropriate sphere of influence is critical for achieving energy and momentum discrimination. In conventional forward propagation, it is common to limit the consideration of third-body forces to only those non-primary objects providing a positionally-significant near-earth orbit perturbation, such as the Moon, Sun and possibly also Jupiter and Mars. However, since energy and momentum are not subject to an inverse distance-squared law, the omission of some intra-solar bodies, even those at great distance from low-earth orbit, will have a deleterious effect on energy and momentum balance. This may result in energy and momentum discrepancies being incorrectly attributed to the primary objects.

The source of state information for non-primary objects also requires care and attention beyond that of conventional forward propagation. Solar planetary ephemerides are built on the interactions of many objects – including over 300 asteroids – as well as post-Newtonian mutual interactions and tidal forces. A planetary ephemeris will also not feature the force, energy and momentum contributions of the primary objects.

2.3 Non-coincident epochs

Arbitrary-precision state information for the two primary objects is highly unlikely to have coincident epochs. For state comparison purposes this is not a disadvantage, but a common start and common end epoch is required for energy and momentum comparisons. Hence, the method features an internal mechanism to forward- or back-propagate states – including the states of the non-primary objects – to bring them into time-coincidence with the epochs of the other primary object.

3 IMPLEMENTATION

The implementation features three conceptual solution layers which assemble the parameter and equation sets into a computational workload of propagations to be performed in a high-performance computing environment, aggregates propagation results into solution matrix elements and solves for the next set of parameter corrections.

3.1 Inner solution layer

Orbital states are initially derived from two-line elements at epoch or higher precision state vectors when available. Gravitational force development includes spherical harmonic earth gravity for the two primary objects and the Moon, and Newtonian point-mass interactions between all other pairings. Ballistic drag is evaluated from a single

coefficient for each primary object in a terrestrial reference frame with a rotating atmosphere. Solar radiation pressure on the primary objects is evaluated using a specular reflection, diffuse reflection and absorption coefficient for each primary object. Solar radiation pressure on the earth is evaluated using the latitude-dependant specular and diffuse properties tabled in [3]. Non-natural forces are evaluated using a trigonometric series of two parameters per band (C1 and C2) plus a constant term (C0) for each axis (R,S,W) and each primary object (o), as shown in Eq. 1. The angular frequency (ω) used is the object's orbital angular frequency. Only one band is used for the results in this paper, therefore in this instance UBN = LBN = 0.

$$F_{\mathrm{o,R,S,W}} = C0_{\mathrm{o,R,S,W}} + \sum_{i=\mathrm{LBN}}^{\mathrm{UBN}} \sqrt{C1^2_{\mathrm{o,R,S,W}} + C2^2_{\mathrm{o,R,S,W}}}\, \sin\left(m\,\omega\,t + atan2\left(C2_{\mathrm{o,R,S,W}}, C1_{\mathrm{o,R,S,W}}\right)\right)$$

$$\text{where } m = \begin{cases} 1 - i & \text{if } i < 0 \\ \frac{1}{i+1} & \text{if } i >= 0 \end{cases}$$

$$\text{and } number\,of\,bands = Upper\,band\,number\,(UBN) - Lower\,band\,number\,(LBN) + 1 \tag{1}$$

Integration is performed by an eighth-order Adams-Bashforth-Moulton predictor-corrector scheme with a correction tolerance of 10^{-9} m kg^{-1} step^{-1}. The inverse proportionality of the mass sets a finer corrector tolerance for heavy non-primary objects that have a greater energy and momentum contribution to the kinematic system. The nominal step size is one second and is adjusted slightly downwards to make an ordinal number of steps fit the required propagation interval. Predictor-corrector schemes are not self-starting, so integrator preambles are developed using the analytical integration of a Lagrange interpolating polynomial.

To achieve high precision integration in the presence of very large total energy and angular momentum – about 10^{35} Joules and 10^{43} kg m^2 s^{-1} respectively – it is necessary to perform arithmetic operations with a 160-bit mantissa, providing 48 significant figures.

3.2 Middle solution layer

The non-primary object states are only drawn from the JPL DE430 planetary ephemeris at the estimated conjunction time. The middle solution layer then performs two subloops to produce cartesian states for the non-primary objects at all epochs, and then back-propagates primary objects to their corresponding opposite epoch. A third subloop then performs the propagation from the primary object starting position to the desired comparison position. Figure 1 shows an example of these subloops in order to perform an energy or momentum comparison spanning the first primary object epoch and the conjunction epoch.

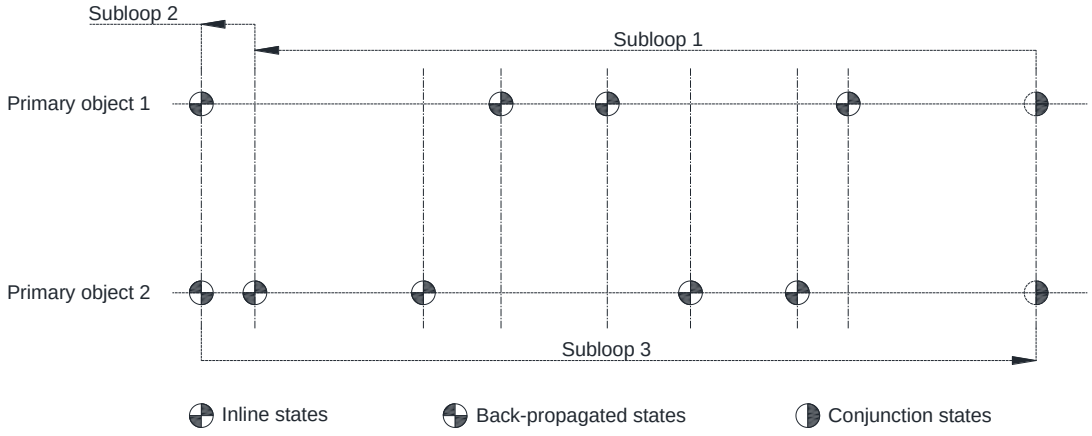

Figure 1. Middle layer subloop operation

First-order finite difference derivatives are obtained for the constituent properties by separately propagating with one perturbed characteristic parameter each. The choice of the finite difference step size is intentionally coarse on the first iteration and is recalculated on subsequent iterations to be the suggested adjustment of the parameter from the previous outer layer correction multiplied by a scaling factor. This negative feedback mechanism prevents large fluctuations in the correction of parameters with very high sensitivities, such as primary object eccentricity.

Equations form rows of derivatives in the solution matrix with the constituent error of that row placed in the corresponding row element of a column matrix. Figure 2 shows possible state geometry comparisons.

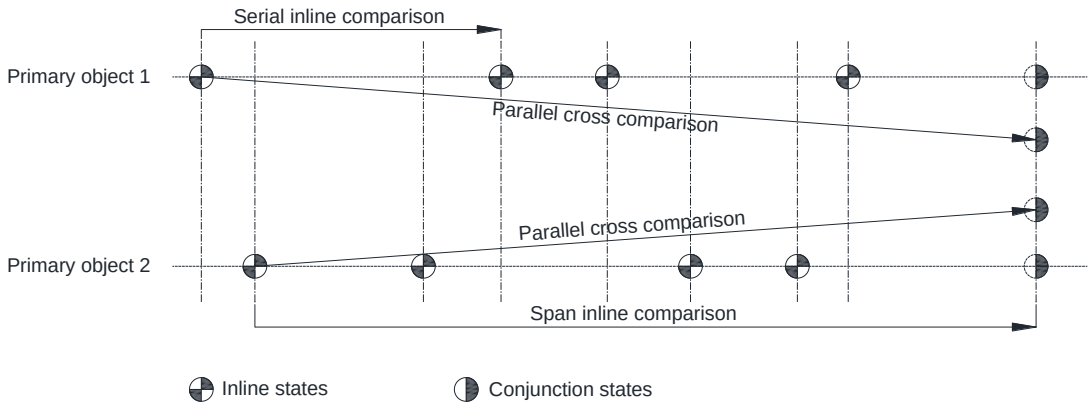

Figure 2. Possible state geometry comparisons

3.3 Outer solution layer

Corrections suggested by the matrix solution are applied to the parameter set iteratively in a relaxed form until converged, which is indicated by vanishing elements in the column matrix, or a vanishing row in the square matrix when the finite difference step size becomes too small to register a movement in a constituent property.

Unlike other cell-based engineering analyses, this method does not produce sparse or banded matrices with row or columns of consistent magnitudes. The solution matrices are typically over two-thirds full of non-zero elements whose minimum to maximum magnitude ranges can be as high as thirty orders across a single row. The solution matrix must be solved using singular value decomposition conducted at IEEE-754 quad precision to prevent internal overflow/underflow. Singular value trimming is performed at 10^{-12} to ameliorate poor matrix condition numbers due to equation non-linearity, particular in the earlier iterations.

3.4 Characteristic parameter set

Throughout most of the development phase, the implementation has been run with four states per primary object. Table 2 shows the current characteristic parameter set, giving a total of 157 parameters.

Table 2. Characteristic parameter set

Parameter	Formation	Number
Primary object states	2 objects x 4 states x 6 elements	48
Conjunction states	2 objects x 6 elements	12
Conjunction time	1 parameter	1
Drag	2 objects x 1 coefficient	2
Solar radiation pressure (SRP)	2 objects x 3 coefficients	6
Primary object mass	2 objects x 1 parameter	2
Primary object spherical radius	2 objects x 1 parameter	2
Generalised discrepancy (GD)	2 objects x 3 axes x 3 coefficients	18
Non-primary object state offsets	11 objects x 6 states	66

3.5 Constituent equation set

Throughout the development phase, the implementation has been run with various constituent equation sets to test their suitability. Table 3 shows the current equation set, giving a total of 157 equations.

Table 3. Constituent equation set

Constituent	Formation	Number
Permuted cross connectivity	2 objects x 2 objects x 4 comparisons x 3 coordinates	48
Serial inline connectivity	2 objects x 4 comparisons x 6 coordinates	48
Serial energy coincidence	2 objects x 4 comparisons	8
Serial angular momentum coincidence	2 epoch times x 4 comparisons x 3 coordinates	24
Span inline connectivity	2 objects x 6 coordinates	12
Span angular momentum coincidence	2 objects x 3 coordinates	6
Span invariant equalisation	2 objects x 3 coordinates	6
Conjunction state equalisation	3 coordinates	3
SRP coefficient normalisation	2 objects	2

There are 4 types of constituent equation suffixes. Connectivity and continuity suffixes are used in state geometry comparisons with cartesian and classical coordinate formulations respectively. Classical state geometry formulation can alleviate some of the non-linearity experienced in cartesian formulation but requires Gauss's variation of parameters to be evaluated at every iteration step, which becomes computationally undesirable.

Coincidence and conservation suffixes are used in energy and angular momentum comparisons. Coincidence and conservation are almost identical except that conservation comparisons allow the contribution of an energy or angular momentum source or sink to be omitted from consideration. This has the effect of driving that source or sink towards minimum contribution. This is of particular importance for the generalised discrepancy function, which should only be permitted to feature forces that do not correlate with other conventional effects such as drag or solar radiation pressure. Conservation equations have not been used in the results in this paper.

The conjunction state equalisation equations are necessary to bring the two supposed primary object conjunction states into positional alignment. The solar radiation pressure coefficient normalisation equations attempt to enforce the requirement that the specular-reflected, diffuse-reflected and absorptive coefficients for each primary object must sum to unity.

4 RESULTS

Final values for the generic discrepancy functions are not shown since they had reached their hard limits before iteration had ceased.

Table 4. Parameter results

Parameter	Object 1	Object 2	Object 3	Object 4	Object 5	Object 6	Units
Drag	1.5	1.5	3.0	1.5	3.0	1.5	
Specular SRP	0.0002	0.99	0.00009	0.999	1.0	1.0	
Diffuse SRP	0.0002	0.99	0.00004	0.001	1.0	1.0	
Absorbed SRP	0.0003	0.99	0.00008	0.001	1.0	1.0	
Mass	998.7	999.9	10	10	999.6	10.2	kg
Radius	1	9.2	10	9.82	10	0.1	m
Conjunction time offset	18.3		-352.5		-12.2		s

Table 5. Constituent results

Constituent	Object 1	Object 2	Object 3	Object 4	Object 5	Object 6	Units
Permuted cross connectivity (initial)	2.449×10^4		2.176×10^4		2.646×10^4		m
Permuted cross connectivity (final)	5.493×10^5		6.925×10^6		9.783×10^5		m
Serial inline connectivity (initial)	7.633×10^3	4.933×10^3	9.043×10^3	6.309×10^3	3.258×10^3	5.984×10^3	m
Serial inline connectivity (final)	2.098×10^3	1.889×10^5	1.022×10^5	3.43×10^6	4.017×10^5	8.852×10^4	m
Serial energy coincidence (initial)	1.163×10^8	1.767×10^8	4.223×10^7	5.77×10^7	1.981×10^7	7.114×10^6	Joules
Serial energy coincidence (final)	1.53×10^9	1.816×10^9	1.918×10^{12}	2.094×10^{12}	1.19×10^{11}	9.103×10^{10}	Joules
Serial angular momentum coincidence (initial)	1.151×10^{15}	1.318×10^{15}	2.777×10^{14}	2.837×10^{14}	1.403×10^{14}	9.904×10^{13}	kg m^2 s^{-1}
Serial angular momentum coincidence (final)	2.499×10^{16}	2.13×10^{16}	1.199×10^{18}	1.251×10^{18}	5.806×10^{16}	4.743×10^{16}	kg m^2 s^{-1}
Span inline connectivity (initial)	1.241×10^4	2.831×10^2	4.376×10^4	1.161×10^4	1.520×10^4	6.779×10^3	m
Span inline connectivity (final)	1.623×10^4	7.032×10^5	1.497×10^6	1.362×10^7	1.354×10^6	6.849×10^5	m
Span angular momentum coincidence (initial)	1.068×10^{15}	1.077×10^{15}	7.496×10^{14}	7.489×10^{14}	5.849×10^{14}	5.832×10^{14}	kg m^2 s^{-1}
Span angular momentum coincidence (final)	9.515×10^{16}	9.537×10^{16}	1.975×10^{18}	1.975×10^{18}	2.786×10^{17}	2.786×10^{17}	kg m^2 s^{-1}
Span invariant equalisation (initial)	2.103×10^2 / 1.1×10^{-5}		1.793×10^2 / 7.96×10^{-6}		2.793×10^2 / 1.204×10^{-5}		m / m s^{-1}
Span invariant equalisation (final)	1.315×10^1 / 5.854×10^{-7}		5.604×10^0 / 2.651×10^{-3}		2.182×10^0 / 2.951×10^{-6}		m / m s^{-1}
Iterations	6		7		9		

5 DISCUSSION

As seen in the results above, very few of the residuals reduced in value over the entire number of iterations, although there were short intervals of downward motion. This may be due to unconstrained parametric movements, particularly the solar radiation pressure coefficients. As shown in Figure 3, the solar radiation pressure coefficient normalisation equations were not strong enough to constrain the sum of the coefficients to unity. This resulted in wide excursions of other related parameters such as mass, radius and the generic discrepancy functions. Strategies to implicitly normalise the solar radiation pressure coefficients are currently being trialled.

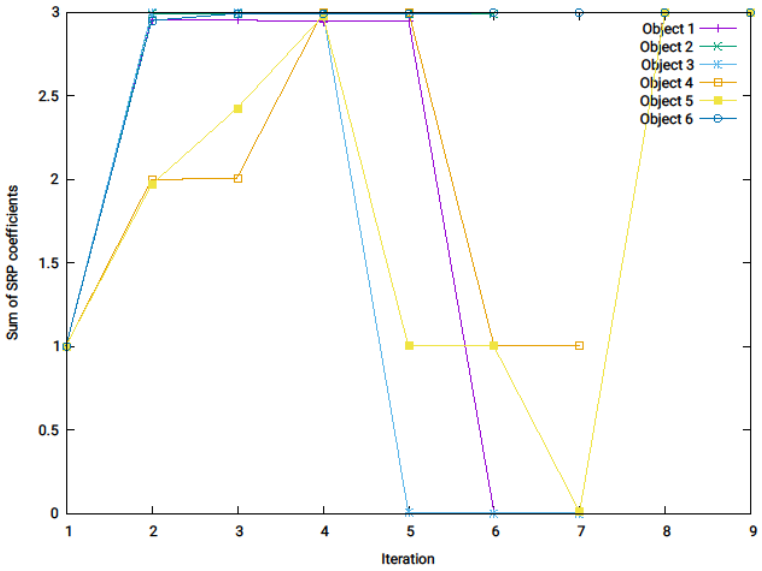

Figure 3. Solar radiation pressure coefficient normalisation

Features to prevent the over-excursion of the generic discrepancy function were trialled during development but those features were found to have insufficient strength. A new strategy to limit generic discrepancy generation to only those perturbations that do not correlate with the other perturbation types is currently sought.

It is possible that the system of equations may be responding adversely to very small derivatives arising from the primary object whose epoch is non-coincident. The mutual gravitational attraction of primary objects is miniscule thereby creating a situation where very large excursions of the non-coincident object might be suggested to perform a constituent residual reduction. Presently, the serial and parallel connectivity of the non-coincident objects do not feature in independent equations and their residuals are not reported. Appropriate equations for these constituents can be added but the corresponding increase in parameters, probably in the generic discrepancy bands, will more than double the computational burden.

6 CONCLUSION

This paper describes the latest implementation challenges that need to be addressed for this method to demonstrate convergence to possibly unique solutions for the collision cases. Work will continue to identify and address the remaining challenges.

7 REFERENCES

1. "*Lost objects*", http:// http://celestrak.com/satcat/lost.php, accessed 8 October 2019.
2. National Aeronautics and Space Administration, "*History of on-orbit satellite fragmentations 15th Edition*", NASA/TM–2018–220037.
3. Knocke P. C., Ries J. C., Tapley B. D., "Earth radiation pressure effects on satellites.", *Proceeding of the AIAA/AAS Astrodynamics Conference*, 88-4292-CP.

8 ACKNOWLEDGEMENT

The author would like to acknowledge the support of the Cooperative Research Centre for Space Environment Management (SERC Limited) through the Australian Government's Cooperative Research Centre Program.